

The Time Scale of Escape from Star Clusters

T. Fukushige

Department of General Systems Studies,
College of Arts and Sciences,
University of Tokyo,
3-8-1 Komaba,
Meguro-ku,
Tokyo 153-8902,
Japan

D.C. Heggie

Department of Mathematics and Statistics,
University of Edinburgh,
King's Buildings,
Edinburgh EH10 5NL,
UK

Abstract

In this paper a cluster is modelled as a smooth potential (due to the cluster stars) plus the steady tidal field of the Galaxy. In this model there is a minimum energy below which stars cannot escape. Above this energy, however, the time scale on which stars escape varies with the orbital parameters of the star (mainly its energy) in a way which we attempt to quantify, with both theoretical arguments and computer simulations. Within the limitations of the model we show that the time scale is long enough to complicate the interpretation of full N -body simulations of clusters, and that stars above the escape energy may remain bound to the cluster for about a Hubble time.

Key words: chaos – gravitation – celestial mechanics, stellar dynamics – globular clusters: general – open clusters: general

1. Introduction

Our initial reason for studying this problem stemmed from a collaborative study of star cluster evolution (Heggie *et al* 1998), the aim of which was to compare results obtained with different codes and models for the same initial conditions. These initial conditions corresponded to a cluster with about 2.5×10^5 stars moving in a circular orbit about a point-mass galaxy. Among the resulting conclusions was a noticeable problem with scaling the results of N -body simulations. (N -body simulations use smaller N than the number of stars in the cluster under study, and so it is necessary to scale the results appropriately.) When this was done on the basis of the theory of relaxation (e.g. Spitzer 1987), the results appeared to depend significantly on N , in the sense that the larger models (i.e. larger N) lost mass more quickly (when scaled to the cluster under study) than smaller models. This

directed our attention to the escape rate from tidally bound clusters with unequal stellar masses.

It turns out that the time scale on which stars escape is one half of the explanation for the scaling problem with the N -body models. The other half of the explanation is the manner in which the initial conditions were set up, which leads to an initial population of stars with energies above the energy of escape (“primordial escapers”). Though all three of the N -body codes that were used in the collaborative experiment were written independently, all three constructed initial models which were inconsistent with the tidal field. In these problems the gravitational field is given by

$$\phi = \phi_c + \frac{1}{2}\omega^2(z^2 - 3x^2), \quad (1)$$

where ϕ_c is the field due to the cluster stars, and the remainder is a combination of tidal and centrifugal terms (cf. Spitzer 1987). In this equation ω is the angular velocity of the cluster round the galaxy, and the coordinates are defined in §2.1. In the N -body simulations initial conditions were set up by first constructing an *isolated* model, and then immersing this in the tidal field. Unfortunately this creates an initial model in which many stars have energy above the escape energy (Fig.1).

This flaw would not matter if these stars with excess energy would escape quickly. It would be possible to wait until they had mostly disappeared, and then examine the relaxation-driven evolution of those that remain. Unfortunately, however, it turns out that the time scale on which these stars escape may be very long, and some do not escape at all (if we take the cluster potential to be fixed). The manner in which the distribution of escape times depends on N is not known, but it evidently complicates the scaling of the models. It was our attempt to understand this problem which motivated our investigation.

Many previous investigations have been devoted to the escape rate of stars from clusters, even if we restrict discussion to those with tidal boundary conditions. Some theoretical investigations (e.g. Chandrasekhar 1943, King 1960, Kwast 1977, Pietrovskaja 1977, Johnstone 1993) actually compute the rate at which stars cross the threshold of *energy* for escape, and it is assumed implicitly that the escape itself is immediate. This remark applies also to estimates from Fokker-Planck models (e.g. Spitzer & Shull 1975, Lee & Goodman 1995), with some exceptions (Lee & Ostriker 1987, Takahashi & Portegies Zwart 1998). Similarly, N -body models have been used to determine escape rates (e.g. Wielen 1975, de la Fuente Marcos 1995) but usually no distinction is made between the time taken to raise the energy of a star above the escape threshold and the time taken to cross the tidal radius.

More apposite to our interests are the simulations of Chernoff & Weinberg (1991), who observed the rate of escape of stars from a cluster in a tidal field, with initial conditions which, like ours, include stars with energy above the escape energy. They found that almost 15% of all the stars escaped beyond a distance of about 3 tidal radii within 100 of their time units, which corresponds to about 500 crossing times, and that stars on prograde orbits escaped slightly faster. Escape is particularly rapid within the first 100 crossing times. This corresponds to roughly the core collapse time of some of the models in the collaborative study already mentioned, which suggests that the continued escape of

stars is a significant complication. Chernoff & Weinberg also measured the rate of loss of particles as a function of energy, a point to which we devote considerable attention in our paper. What complicates the interpretation of their results for our purposes, however, is the fact that many stars were initially outside the tidal radius, and also we are interested in escape across the tidal radius, rather than some larger radius.

The simulations of Baumgardt (1997) and Johnston, Sigurdsson & Hernquist (1999) take this kind of study further by placing the cluster on an eccentric galactic orbit. In the present paper, however, we restrict attention to the circular case, with which the collaborative experiment was also concerned.

Our aim is to study the distribution of escape times, as a function of energy, for stars initially located inside the tidal radius. In addition to the results of new numerical simulations not unlike those of Chernoff & Weinberg (Section 2), we provide some information on how these results depend on the initial cluster model. We also show that it is possible to give some theoretical estimates of the escape time scale and its energy dependence (Section 3), which are compared with our numerical results in Section 4. Section 5 summarises our conclusions and applies them to a number of results in the literature.

2. Numerical Results

2.1 Method

We calculated the orbits of stars in a smoothed potential due to cluster stars plus the steady tidal field of the Galaxy, in order to obtain the escape time from the cluster. We set the initial center of mass of the cluster at the origin $(x, y, z) = (0, 0, 0)$ with axes oriented so that the position of the galactic center is $(-R_g, 0, 0)$. We assumed that the size of the cluster is much smaller than R_g . If the cluster revolves around the galactic centre at constant angular velocity $\boldsymbol{\omega} = (0, 0, \omega)$, the equation of motion of a star can be expressed as

$$\frac{d^2\mathbf{r}}{dt^2} = -\nabla\phi_c(r) - 2\boldsymbol{\omega} \times \frac{d\mathbf{r}}{dt} + \omega^2(3x\mathbf{e}_x - z\mathbf{e}_z), \quad (2)$$

where \mathbf{r} is the position of the star, and $\mathbf{e}_x, \mathbf{e}_z$ are unit vectors that point along the x and z axes, respectively.

The first term on the right-hand side in eq.(2) is the gravitational acceleration from the cluster. We used King's models (King 1966) for the potential of the cluster, and the potential is smooth and fixed. We used standard units such that $M = G = -4E_c = 1$, where M is the total mass of the cluster, G is the gravitational constant, and E_c is the total self-energy of the cluster (Heggie and Mathieu 1986). We performed calculations with King models which differ in the dimensionless central potential, $W_0 = 3, 7, 12$. In order to compute the acceleration of the King model, we used cubic spline interpolation between data obtained by numerical solution (e.g. Press et al. 1992).

The second term on the right-hand side in eq.(2) is the Coriolis acceleration, and the third term is a combination of the centrifugal and tidal forces. Here we assumed that the cluster moves on a circular orbit in a spherically symmetric galactic potential, taken to be that of a distant point mass. The angular velocity, ω , is given by

$$\omega = \sqrt{\frac{GM}{3r_t^3}} \quad (3)$$

where r_t is the tidal radius of the cluster. We set r_t to be equal to the tidal radius of the King model, and so obtained ω .

We calculated orbits of 1000 stars to obtain the distribution function of escape time, for several values of the dimensionless energy excess, $\tilde{E} = (E - E_{\text{crit}})/|E_{\text{crit}}|$, where E is the energy of a star of speed v , given by

$$E = \frac{v^2}{2} + \phi_c + \frac{1}{2}\omega^2(z^2 - 3x^2),$$

and E_{crit} is the potential at the Lagrangian points, given by

$$E_{\text{crit}} = -3GM/2r_t. \quad (4)$$

(Fig.2). The criterion of escape is simply geometric: escapers are defined to be those stars beyond the tidal radius.

We performed calculations of orbits from two kinds of initial spatial distribution of stars: a “uniform” distribution, and a “King” or “non-uniform” distribution. In the former distribution, the positions of stars are distributed uniformly inside the tidal radius of the cluster. In the latter distribution, the positions of the stars are distributed in the same way as the primordial escapers in a King model immersed in the tidal field. In this case the stars tend to be distributed in the inner regions of the cluster due to the decrease of the potential by the tidal field in the outer region (see Fig.1). In either case the velocity is distributed isotropically, and its magnitude is determined by the given value of \tilde{E} .

We integrated the orbits of the stars by means of a fourth-order Hermite integration scheme (Makino & Aarseth 1992) with a variable time step algorithm. The integration error in energy was about 5×10^{-3} at most, and typically of order 10^{-3} at the point where the longest simulation was stopped ($t = 8 \times 10^5$, $W_0 = 3$, $\tilde{E} = 0.03$). The error varied almost linearly with time. Conversely, the point at which integrations were stopped, and the smallest value of \tilde{E} , were determined from the maximum error.

2.2 Results

A typical result is given in Fig.3. It shows the distribution of escape times from a King model with $W_0 = 3$, when the initial conditions are selected as in the collaborative experiment (i.e. a “King” distribution, cf.§2.1). Results are presented for different values of the stellar energy, in terms of \tilde{E} .

The integrations were terminated at some large time, corresponding to the vertical lines at the right side. Even so, it is clear that there is a significant fraction of initial conditions for which the escape time is effectively infinite. This fraction decreases with increasing energy excess \tilde{E} , and varies somewhat from one model to another (Fig.4). In the case of non-uniform initial conditions with $W_0 = 3$ (i.e. the dashed line with triangles) the decrease is perhaps distorted by the fact that the termination times of the runs with different \tilde{E} are different. Empirically, the fraction of non-escapers is about $f_n \simeq 0.17 - 0.6\tilde{E}$ for uniform initial conditions and about $0.26 - 0.9\tilde{E}$ for non-uniform conditions. Further inspection of our results showed that a majority of these non-escapers are in retrograde orbits initially, i.e. the sense of their motion around the cluster is the same as the sense of motion of the cluster about the galaxy.

Now we turn attention to the particles which escaped within the time limit of the simulations. The escape time decreases with increasing \tilde{E} . For the example shown in Fig.3 the median escape time (i.e. $P = 0.5$) decreases by approximately two orders of magnitude as \tilde{E} increases from 0.03 to 0.24. For a given \tilde{E} the escape time is slightly smaller for uniform than for non-uniform initial conditions. Presumably part of the reason for this is that a larger fraction of initial conditions lie at large radii for uniform initial conditions. For non-uniform initial conditions the escape time decreases slightly with increasing W_0 , presumably for the same reason, at least in part. This is not a complete explanation, however, as there is also a decrease of escape time with increasing W_0 when the initial conditions are sampled uniformly.

We postpone further discussion of these results until some theoretical considerations have been developed in the following section.

3. Theory

3.1 Overall escape rate

The Lagrange points are saddle points of the effective potential, and when the energy E is just above E_{crit} , a star must pass close to one of these saddles in order to escape. It is not difficult to compute an upper bound on the rate at which phase volume crosses each of the surfaces $x = \pm r_t$ in phase space, and hence an upper bound on the escape rate follows if we know the phase density of stars. The calculation is a simple case of a more general theoretical result about flow near saddles (MacKay 1990), but the proof we give is more pedestrian.

Shifting the origin to a saddle point and expanding to second order, we find that

$$\phi - E_{\text{crit}} = \frac{1}{2}\omega^2(-9x^2 + 3y^2 + 4z^2). \quad (5)$$

The one-way flux of phase volume, per unit energy, across $x = 0$ is simply

$$\mathcal{F} = \int_{\dot{x}>0} \delta(\phi + \frac{1}{2}(\dot{x}^2 + \dot{y}^2 + \dot{z}^2) - E) \dot{x} d\dot{x} d\dot{y} d\dot{z} dy dz. \quad (6)$$

where ϕ is evaluated at $x = 0$. The integrations are readily done, but we must double the result as there are two saddles past which stars can escape. The final answer is thus

$$\mathcal{F} = \frac{2\pi^2(E - E_{\text{crit}})^2}{\sqrt{3}\omega^2}. \quad (7)$$

A familiar calculation shows that the phase space volume per unit energy is $\mathcal{V} = 4\pi \int \sqrt{2(E - \phi)} d^3\mathbf{r}$ over the appropriate domain in space. This does not depend sensitively on E in the vicinity of $E = E_{\text{crit}}$, and so we evaluate it there. The integration may be estimated by a Monte Carlo technique, but in this section we approximate ϕ_c with the potential of a point mass, and then the integrand is mildly unbounded. This can be handled by writing the integrand as $\sqrt{2(E - \phi)} r r^{-1/2}$, where $r^2 = \mathbf{r} \cdot \mathbf{r}$, and sampling points with density proportional to $r^{-1/2}$. Our result is

$$\mathcal{V} = 4\pi C \sqrt{2} (GM)^{4/3} \omega^{-5/3}, \quad (8)$$

where $C = 0.40 \pm 0.01$. It follows that the time scale for escape of phase volume is

$$t_e = \frac{\mathcal{V}}{\mathcal{F}} = \frac{2C\sqrt{6}}{\pi} \frac{(GM)^{4/3}\omega^{1/3}}{(E - E_{\text{crit}})^2}, \quad (9)$$

or, in dimensionless form, $\omega t_e = \frac{2^{7/2}C}{3^{13/6}\pi\tilde{E}^2}$.

In order to turn this result into an estimate of the time scale of the escape of stars, there are two issues to be addressed. One is the distribution of stars within phase space, the effect of which was discussed from a numerical point of view in Sec.2.2. The second is the fact that eq.(7) is strictly only an upper limit on the escape rate, which we consider qualitatively in the next section.

It is worth noting that there is an appealing “physical” argument for the escape rate which nevertheless leads to a wrong answer. In the coordinates of eq.(5), it is clear that an escaping star must pass through an elliptical aperture at $x = 0$ with semi-axes $\sqrt{2(E - E_{\text{crit}})}/3/\omega$ and $\sqrt{(E - E_{\text{crit}})}/2/\omega$, respectively. There are two such apertures, and their total area is a fraction $\frac{E - E_{\text{crit}}}{2\sqrt{3}\omega^2 r_t^2}$ of the area of a sphere of radius r_t . If we assume that this fraction of the stars find their way through one of these apertures in each crossing time, which is of order $2\pi/\omega$, we find that the time scale of escape varies as $(E - E_{\text{crit}})^{-1}$, in contrast with eq.(9). Presumably what is missing is the condition that the star should approach the aperture from the correct direction.

Actually, there is a correct physical interpretation of these results, though not an intuitive one. In the two-dimensional problem of motions in the plane $z = 0$, we see from eq.(6) that

$$\mathcal{F} = \oint \dot{y} dy, \quad (10)$$

where $\phi + \dot{y}^2/2 = E$. This expression for \mathcal{F} resembles an action integral. In fact it is the action of an unstable periodic orbit situated close to the L_1 (saddle) point (cf.§3.2.2). We are not aware, however, of any comparable interpretation of the three-dimensional result, i.e. eq.(7).

3.2 Qualitative Results on Escape

3.2.1 Non-Escapers

Let us consider the case of motion in the x, y plane, and again take $\phi_c = -GM/r$. We change to units in which $GM = \omega = 1$. Fig.5 shows the surface of section $y = 0$ (with coordinates x, \dot{x}) for motions of energy E_{crit} , and the curve $\dot{y} = 0$. More than half of the surface is occupied by apparently regular orbits when $E = E_{\text{crit}}$, and the proportion does not decrease dramatically if E exceeds E_{crit} slightly. Such stars would not escape. It is not clear whether the same conclusion applies in the three-dimensional problem, because of Arnold diffusion. Nevertheless it is plausible that these apparently regular motions correspond approximately to the stars which do not escape in the numerical simulations of Sec.2.2. The presence of such stars implies that eq.(9) overestimates the escape time scale, because eq.(8) overestimates the volume of phase space that can escape.

Incidentally, the regular orbits correspond mainly to retrograde motions, i.e. motions in which the star revolves around the cluster in the opposite sense to the motion of the cluster around the galaxy. The stability of such motions is well known in analogous problems (e.g. Benest 1974, Keenan & Innanen 1975, Huang & Innanen 1983, Ross, Mennim & Heggie 1997). The range of such orbits has been studied numerically for the planar problem with a point-mass potential by Hénon (1970) and Brunini (1996), and for a cluster-like potential by Jefferys (1976). He found that the measure of permanently bound orbits decreases with increasing energy, and is negligibly small for $\tilde{E} \gtrsim 0.3$.

3.2.2 Escapers

So far we have seen that stars with a given energy above the escape energy appear to fall into two kinds, depending on whether or not they eventually escape. Now we consider those that do eventually escape. As shown long ago by Hayli (1970), it is clear that such stars must closely approach one or other Lagrange point, and pass the narrow neck which opens out in the surface of section of Fig.5 when $E > E_{\text{crit}}$. It will be useful to consider some features of the orbits within this region. We concentrate on motions in the x, y plane, but qualitatively similar conclusions follow for three-dimensional motions.

The Lagrange points exist precisely at $E = E_{\text{crit}}$, but at $E > E_{\text{crit}}$ there is an unstable periodic orbit situated close to each of these points (cf. Hénon 1969 and the Appendix). This orbit shrinks to the unstable equilibrium point as $E \rightarrow E_{\text{crit}}+$. In the present context it exerts a strong controlling influence on would-be escapers, as we shall see.

Precisely at E_{crit} there is only one orbit that approaches the equilibrium point as $t \rightarrow \infty$ (Fig.6). At each slightly higher energy there is a one-parameter family of orbits approaching the periodic orbit (at different “phases”). Fig 7 shows one of these. In phase space the set of all such orbits (at fixed energy) forms a tubular surface*. Fig.8 shows the final section of several such orbits, and there are enough to allow the tube (or at least its projection onto the x, y plane) to be visualised. By examining the equations of motion in the vicinity of the Lagrangian point, it is not hard to see that it is orbits *inside* this tube which lead to escape. Indeed the flux of phase space along this tube is equal to the value in eq.(10). This tube is rather like a hose connecting the interior of the cluster (at least, the section in the x, y plane) with the outside world.

If we follow backwards the tube of orbits leading to the periodic orbit we see that it must approximately follow the orbit shown in Fig.6. It lies roughly within the region of the surface of section which, at energy E_{crit} (Fig.5), is occupied by chaotic orbits. It is reasonable to conjecture that the tube, as it is followed backwards, becomes increasingly distorted and convoluted within this region of apparently chaotic motions. Consideration of phase space volume immediately shows, however, that the tube cannot remain in this region indefinitely. Increasingly it must connect with the region outside the cluster, corresponding to motions which are temporarily captured within r_t . Indeed the time scale on which this happens must be of order t_e , given by eq.(9) for the three-dimensional problem. Returning to the direction in which time increases, we see that stars can enter the cluster from outside, remain within the cluster (inside the tube) for some time, and then escape again.

* In dynamical systems theory this is called the *stable invariant manifold* of the periodic orbit

3.2.3 The Distribution of Escape Times

Now we can construct a qualitative picture of the rate at which stars escape. Consider an experiment in which stars are distributed within the cluster at some energy above E_{crit} . (The numerical results of such experiments are described in Sec.2.) Some of these stars will lie in the regular region of phase space (Fig.5), and never escape. Others will lie within the tube of escapers, and will initially escape at a rate given by eq.(7), multiplied by their density in phase space. On a time scale of order t_e , however, the rate of escape will diminish, as the phase space which escapes consists increasingly of parts of phase space which have been temporarily captured from outside.

This picture can be given considerable precision in the language of chaotic transport (Wiggins 1992), though it is beyond the scope of this paper. This theory, combined with appropriate numerical results, permits a computation of the manner in which the rate of escape diminishes with time, which in turn is determined by the distribution of escape times. In some model problems the distribution of escape times is approximately exponential, and in others it is approximately a power law. The division into non-escapers and escapers, with a power-law distribution of escape times for the latter, is also found in numerical studies of other idealised escape problems (Kandrup *et al* 1999).

There is one situation where we may estimate the distribution of escape times rather easily. Consider first an orbit on the surface of the tube which approaches the Liapounov orbit as $t \rightarrow \infty$: its escape time is infinite. An orbit just inside the surface of the tube spends a long time close to the Liapounov orbit, before eventually escaping. In fact, from familiar estimates of flow near a saddle point, it is easy to see that the escape time varies nearly as $\ln(1/d)$, where d is the distance of the orbit from the surface of the tube. This leads to an exponential distribution of escape times. Though it seems that this argument applies only to orbits lying close to the tube, we have argued that this tube is highly convoluted throughout a large region of phase space, which would imply that the resulting distribution of escape times is more widely applicable.

The problem of the distribution of escape times is actually a good deal more complicated. There are in fact *two* places (corresponding to the two Lagrangian points) where stars may escape from the cluster. Each has its own “tube” of orbits with infinite escape times, though it is not clear to what extent these two tubes are intertwined with each other. Further complexity is added by motions which are asymptotic to other periodic orbits inside the cluster. Some of these orbits and the associated complexity may be glimpsed in the numerical calculations of Murison (1989), who computed the *capture* times of a large number of orbits in a similar problem. By time-reversibility, however, similar conclusions can be reached about escape times.

In other dynamical problems (e.g. the breakup of triple systems, cf. Anosova & Orlov 1994) the rate of escape diminishes approximately exponentially with time. Despite the complications, then, we may at least *conjecture* similar behaviour in the present problem, on the basis of little more than the above simplified arguments and analogies. The empirical evidence will be considered in the next section.

4. Interpretation of Numerical Results

We first consider the predicted dependence on \tilde{E} of the escape time scale, i.e. $t_e \propto \tilde{E}^{-2}$ (eq.[9]), taking the data of Fig.3 as an example. If we exclude the particles which have not

escaped at the end of each set of computations, and scale the escape time to

$$\tilde{t} = \omega t \tilde{E}^2, \quad (11)$$

the result is Fig.9. After an early transient the approximate coincidence of the curves is a measure of the success of the predicted energy dependence.

In order to analyse this data we fitted a model based loosely on the theory of §3. If we assume that stars escape on a time scale t_e then

$$P(t) = \exp(-t/t_e) \quad (12)$$

and $P(\tilde{t}) = \exp(-\tilde{t}/\tilde{t}_e)$, where \tilde{t}_e is defined in the obvious way. If \tilde{t}_e is taken from eq.(9), the result is plotted as the dashed line in Fig.9. As can be seen this is a hopelessly poor fit: the time scale is too short by about 1 dex. Recall, however, that this theory was derived from arguments of escape of phase space from the field of a point mass, whereas phase space is sampled non-uniformly in the numerical data and the potential is far from that of a point mass. Both factors compare better if we turn to high-concentration models and a uniform distribution of initial conditions, and then the predicted time scale agrees much better.

Even if \tilde{t}_e is treated as an arbitrary parameter (corresponding to horizontal translation in Fig.9) the fit is not entirely satisfactory: both tails of the distribution are not well described. For this reason we have also tried the empirical distribution $P(\tilde{t}) = (1 + a\tilde{t})^{-b}$, where a, b are adjustable constants. The result is shown as a solid line in Fig.9. It is quite satisfactory. Incidentally, the data curve which is most deviant at large \tilde{t} has the smallest value of \tilde{E} , where the effect of the finite cutoff in t in the numerical integrations is likely to be most serious. The best fitting parameters from all sets of data are given in Table 1. The quality of the fit is comparable to that in Fig.9 for all cases except $W_0 = 3$ and uniform initial conditions. Also shown in this Table is the time $\tilde{t}_{1/2}$ at which $P = 1/2$. This illustrates the trends mentioned in connection with eqs.(9) and (12), for which $\tilde{t}_{1/2} \simeq 0.092$: the result is smaller for larger W_0 and uniform initial conditions.

For the non-escapers the interpretation of the numerical results is less quantitative. The fact that the majority of non-escapers move initially on retrograde orbits is consistent with the known stability of retrograde motions (§3.2.1). The approximate limit of $\tilde{E} = 0.3$ (for the planar problem) is approximately in line with Fig.4. Nevertheless this Figure refers to the three-dimensional problem, and we also find that significant numbers of non-escapers exhibit prograde motion. An example is shown in Fig.10. Note that this is a cross section in *configuration* space, i.e. it is not a Poincaré surface of section. (Actually there is also a tiny fraction of stable prograde orbits even in the planar problem, as one can just discern in Fig.5.) The sharply defined outer boundary of the plot in Fig.10 suggests a regular orbit, and is a very common feature of such plots for non-escapers, both prograde and retrograde.

These features contrast sharply with those for escapers. Fig.11 illustrates a similar plot for one of the longest lasting escapers. Note the absence of sharp boundaries, suggesting an effectively stochastic orbit. Further study showed that this orbit spends a long time in a restricted part of phase space, corresponding to the denser part of the distribution. At early and late times, however, its distribution was wider.

5. Discussion and Conclusions

It was mentioned in the introduction that this was our motivation for studying the distribution of escape times. The main numerical results were given in Sec.2 as a function of the energy of a star. In a model star cluster, however, the primordial escapers have a range of energies, and we have carried out similar calculations for this distribution. For a King model with $W_0 = 3$ we found that the fraction of stars which were “primordial escapers” was 0.137 ± 0.003 (90% confidence), and that their median time of escape was 1360 ± 180 N -body units.

Now let us compare this with the lifetime of a simulation. Here we take the initial parameters of the “collaborative experiment” (Heggie *et al* 1998), in which the initial mass function was of the Salpeter form, i.e. $f(m)dm \propto m^{-2.35}dm$, with a range of masses which scales to $0.1M_\odot < m < 1.5M_\odot$. The time t_h for half of the mass to escape beyond the tidal radius is given in Table 2, for one of the participating groups. We also give the fraction F of all stars which were primordial escapers and which would have remained within the tidal radius at t_h , assuming that the potential had not evolved.

From these results we see that the time scale on which the primordial escapers leave the cluster is at least comparable with the time scale on which it loses mass. It is this process which makes scaling of these results problematic. The time scale for loss of primordial escapers is approximately independent of N , whereas the two-body relaxation time scale is approximately proportional to N (except for the Coulomb logarithm). If the time scale of escape had been very short, it might have been possible to create appropriate initial conditions by running the model for a short time, during which the escapers leave but the effects of relaxation are still minor.

In some N -body calculations (e.g. Portegies Zwart *et al* 1998) the tidal effect is treated as a *cutoff*, i.e. stars are removed as soon as they cross the radius r_t , though the equations of motion ignore all but the first term in eq.(2). This procedure avoids the difficulty of setting up self-consistent initial conditions. By a calculation analogous to that in Sec.3.1, the time scale for escape of phase volume across the tidal boundary changes to

$$t_e = \frac{\pi}{8} \frac{\sqrt{-2E_{\text{crit}}r_t}}{E - E_{\text{crit}}},$$

where now $E_{\text{crit}} = -GM/r_t$. The important change is in the dependence on $(E - E_{\text{crit}})$: stars with energy just above the escape energy (which may result from two-body encounters in a cluster, for example) escape much more readily with a tidal cutoff than with a tidal field. On the other hand these models also do not contain any primordial escapers, and so the benefit of a short escape time scale is not so necessary for scaling purposes.

To return to the case of a tidal field, it is clear that scaling the results of N -body simulations requires rather detailed modelling of the escape process, and relevant data for such a task are presented in this paper. On the other hand we have considered a simpler problem, as the potential is fixed. In an N -body simulation the potential alters as the cluster loses mass. In addition, the primordial escapers are supplemented by stars which gain enough energy to escape by two-body encounters. The theory of relaxation

implies that the energy which they have at this point depends on N , and therefore the determination of the time scale on which they escape is a more complicated problem.

Since relaxation is a diffusive process, it can be argued that the energy which a star reaches before escaping, if the time taken is t_e , is given by an expression which scales as $E - E_{\text{crit}} \sim E_{\text{crit}}(t_e/t_r)^{1/2}$, where t_r is the relaxation time. Since we also have

$$t_e \sim \frac{1}{\omega} \left(\frac{E_{\text{crit}}}{E - E_{\text{crit}}} \right)^2,$$

by eqs.(3), (4) and (9), it follows that $t_e \sim \sqrt{t_r/\omega}$, i.e. the typical escape time varies as the geometric mean of the crossing and relaxation times.

Besides the collaborative experiment to which we have referred, there are many simulations in the literature whose interpretation may be complicated by the presence of primordial escapers, and which have usually gone unnoticed. For example Wielen (1975) found that the mass-dependence of the escape rate on stellar mass was much weaker than expected theoretically; this could be expected if a substantial number of escapers was primordial, though other factors referred to by Wielen (such as mass segregation) surely also play a role. Sugimoto & Makino (1989) studied the evolution of binary clusters by placing two concentrated King models in a circular relative orbit, and drew attention to the importance of escape for driving the clusters together. The results of Fukushige & Heggie (1995) on the dissolution of tidally limited clusters by mass loss from stellar evolution, and those by Vesperini & Heggie (1997) on the effect of dynamical evolution on the mass function, are also subject to the effects of primordial escapers.

When the escape time scales found in Secs.2 and 5.1 are scaled to real clusters, it is found that the escape time scales can be surprisingly long. For example, in a King model with $W_0 = 3$ at a galactocentric distance R_g in a galaxy with circular speed V , the median escape time is about $6 \times 10^9 \left(\frac{R_g}{10\text{kpc}} \right) \left(\frac{220\text{km/sec}}{V} \right)$ yr. Furthermore, we have seen that it is possible for stars to remain inside the tidal radius indefinitely, even with energies above the energy of escape. Now in two clusters a few stars have been observed with radial velocities surprisingly close to the escape velocity of a dynamical model (Gunn & Griffin 1979, Meylan, Dubath & Mayor 1991). Usually interpreted as ejecta from energetic interactions in the core (Davies, Benz & Hills 1994, Sigurdsson & Phinney 1995), or perhaps as evidence of a centrally condensed population of dark remnants (Larson 1984), it is possible that they are simply trapped within the cluster with energies above the escape energy.

It must be remembered that our results apply to an idealised problem, and in particular to a cluster on a circular galactic orbit. On the other hand Johnston *et al* (1999) have pointed out that clusters may be accompanied by an *extratidal* population of bound stars even in the elliptic case, and so the existence of such stars within the tidal radius is perfectly plausible. It is also not hard to see how such orbits can be populated: at any stage a cluster will contain stars on retrograde orbits at energies below the energy of escape; as the cluster loses mass their energy will increase, placing them in retrograde orbits within the cluster but above the escape energy.

Acknowledgements

T.F. acknowledges financial support from the “Research for the Future” Program of the Japan Society for the Promotion of Science, grant no. JSPS-RFTP 97P01102, and thanks Jun Makino for helpful discussions.

References

- Anosova J.P., Orlov V.V., 1994, CeMDA, 59, 327
Baumgardt H., 1997, PhD Thesis, University of Heidelberg (in German)
Benest D., 1974, A&A, 32, 39
Brunini A., 1996, in Muzzio J.C., Ferraz-Mello S., Henrard J., eds, Chaos in Gravitational N -Body Systems. Kluwer, Dordrecht, p.79
Chandrasekhar S., 1943, ApJ, 97, 54
Chernoff D.F., Weinberg M.D., 1991, in Janes K., ed, ASP Conf. Ser. 13, The Formation and Evolution of Star Clusters. ASP, San Francisco, p.373
Davies M.B., Benz W., Hills J.G., 1994, ApJ, 424, 870
de la Fuente Marcos R., 1995, A&A, 301, 407
Fukushige T., Heggie D.C., 1995, MNRAS, 276, 206
Gunn J.E., Griffin R.G., 1979, AJ, 84, 752
Hayli A., 1970, A&A, 7, 17
Heggie D.C., Giersz M., Spurzem R., Takahashi K., 1998, in Andersen J., ed, Highlights of Astron., Vol.11B. Reidel, Dordrecht, p.591
Heggie D.C., Mathieu R.D., 1986, in Hut P., McMillan S., eds, LNP267, The Use of Supercomputers in Stellar Dynamics. Springer-Verlag, Berlin, p.233
Hénon M., 1969, A&A, 1, 223
Hénon M., 1970, A&A, 9, 24.
Huang T.-Y., Innanen K.A., 1983, AJ, 88, 1537
Jefferys W.H., 1976, AJ, 81, 983
Johnston K., Sigurdsson S., Hernquist L., 1999, MNRAS, 302, 771
Johnstone D., 1993, AJ, 105, 155
Kandrup H.E., Siopis C., Contopoulos G., Dvorak R., 1999, astro-ph/9904046
Keenan D.W., Innanen K.A., 1975, AJ, 80, 290
King I.R., 1960, AJ, 65, 122
King I.R., 1966, AJ, 71, 64
Kwast T., 1977, Post. Astron, 25, 105
Larson R.B., 1984, MNRAS, 210, 763
Lee H.-M., Goodman J., 1995, ApJ, 443, L109
Lee H.-M., Ostriker J.P., 1987, ApJ, 322, 123
MacKay R.S., 1990, Phys. Lett. A, 145, 425
Makino J., Aarseth S.J., 1992, PASJ, 44, 141
Meylan G., Dubath P., Mayor M., 1991, ApJ, 383, 587
Murison M.A., 1989, AJ, 98, 2346 and 2383
Petrovskaja I.V., 1977, Post. Astron., 25, 59
Portegies Zwart S.F., Hut P., Makino J., McMillan S.L.W., 1998, A&A, 337, 363
Press W.H., Teukolsky S.A., Vetterling W.T., Flannery B.P., 1992, Numerical Recipes, 2nd ed. Cambridge Univ. Press, Cambridge

- Ross D.J., Mennim A., Heggie D.C., 1997, MNRAS, 284, 811
 Sigurdsson S., Phinney E.S., 1995, ApJS, 99, 609
 Spitzer L., Jr, 1987, Dynamical Evolution of Globular Clusters. Princeton Univ. Press, Princeton
 Spitzer L., Jr, Shull J.M., 1975, ApJ, 201, 773
 Sugimoto D., Makino J., 1989, PASJ, 41, 1117
 Takahashi K., Portegies Zwart S.F., 1998, ApJ, 503, L49
 Vesperini E., Heggie D.C., 1997, MNRAS, 289, 898
 Wielen R., 1975, in Hayli A., ed, Proc. IAU Symp. 69, Dynamics of Stellar Systems. D. Reidel, Dordrecht, p.119
 Wiggins S., 1992, Chaotic Transport in Dynamical Systems. Springer-Verlag, New York

Appendix: Motion near a Lagrangian Point

Adding the Coriolis acceleration (the cross product in eq.(2)) to the acceleration derived from eq.(5), and choosing units in which $\omega = 1$, we have the linearised equations of motion

$$\begin{aligned}\ddot{x} - 2\dot{y} - 9x &= 0 \\ \ddot{y} + 2\dot{x} + 3y &= 0.\end{aligned}$$

Their general solution is

$$\begin{pmatrix} x \\ y \end{pmatrix} = A \begin{pmatrix} -\mu \\ 4 - \sqrt{7} \end{pmatrix} \exp \mu t + B \begin{pmatrix} \mu \\ 4 - \sqrt{7} \end{pmatrix} \exp[-\mu t] + C \begin{pmatrix} -\nu \cos(\nu t + \theta) \\ (4 + \sqrt{7}) \sin(\nu t + \theta) \end{pmatrix},$$

where $\mu = \sqrt{1 + 2\sqrt{7}}$, $\nu = \sqrt{2\sqrt{7} - 1}$ and A , B , C and θ are arbitrary constants. The energy is $E = E_{\text{crit}} + C^2(10\sqrt{7} + 49) + AB(196 - 40\sqrt{7})$.

When $A = B = C$ we have equilibrium at the Lagrange point; when only C is non-zero we have a linear approximation to the periodic orbit referred to in Sec.3.2.2; when also B is non-zero we have a local approximation to an orbit which approaches the periodic orbit asymptotically.

Tables

Table 1
 Empirical fit to distribution of \tilde{t}

W_0	Initial conditions	a	b	$\tilde{t}_{1/2}$
3	Non-uniform	1.80	0.869	0.680
3	Uniform	7.68	0.579	0.301
7	Non-uniform	3.96	0.758	0.377
7	Uniform	8.31	0.729	0.191
12	Uniform	5.98	0.914	0.189

Table 2

Half-Mass Time for one set of N -body Results of the Collaborative Experiment

N	4096	8192	16384	32768
t_h	260	410	620	1000
F	0.093 ± 0.005	0.087 ± 0.005	0.080 ± 0.005	0.073 ± 0.003

Note: the times are given in N -body units (Heggie & Mathieu 1986), as in Section 2.

Figure Captions

Fig.1 Creation of a cluster model with a tidal radius of 2 (in suitably scaled units). The solid curve shows the potential well of an isolated model, and stars are created with energies up to the solid horizontal line. Then the galactic tide (long-dashed) is added. This creates a tidal radius at the maximum of the combined potential (lower dashed curve), but the stars have energies up to the upper dashed curve. Many lie above the escape energy (corresponding to the value of the combined potential at the tidal radius.)

Fig.2 Equipotentials of the effective gravitational potential ϕ experienced by a star in a tidally limited cluster, including the inertial force caused by the rotation of the frame of reference about the galactic centre. The cluster potential is approximated by that of a point mass, and units are such that $\phi = -1/\sqrt{x^2 + y^2} - 3x^2/2$ in the plane $z = 0$. The Lagrange points are the saddle points.

Fig.3 Cumulative distribution of escape times from a King model with $W_0 = 3$. P is the probability (i.e. fraction of initial conditions) that the lifetime exceeds t . The initial conditions are selected non-uniformly, as explained in the text. The relative excess energy is, from left to right, $\tilde{E} = 0.24, 0.16, 0.12, 0.08, 0.06, 0.04$ and 0.03 .

Fig.4 Fraction of initial conditions with “infinite” escape time, i.e. “non-escapers”, if the potential is fixed. The initial conditions stated in the key are described in Sec.2.1.

Fig.5. Surface of section for motion in the x, y plane at energy E_{crit} . Each point corresponds to the value of x and \dot{x} at the instant when the orbit crosses the y -axis with $\dot{y} > 0$. Different orbits are characterised by different symbols.

Fig.6. The orbit asymptotic (as $t \rightarrow \infty$) to the Lagrangian point $x = r_t$ (in units with $G = M = \omega = 1$).

Fig.7. An orbit asymptotic to a periodic orbit (at the right of the figure), at some energy above E_{crit} .

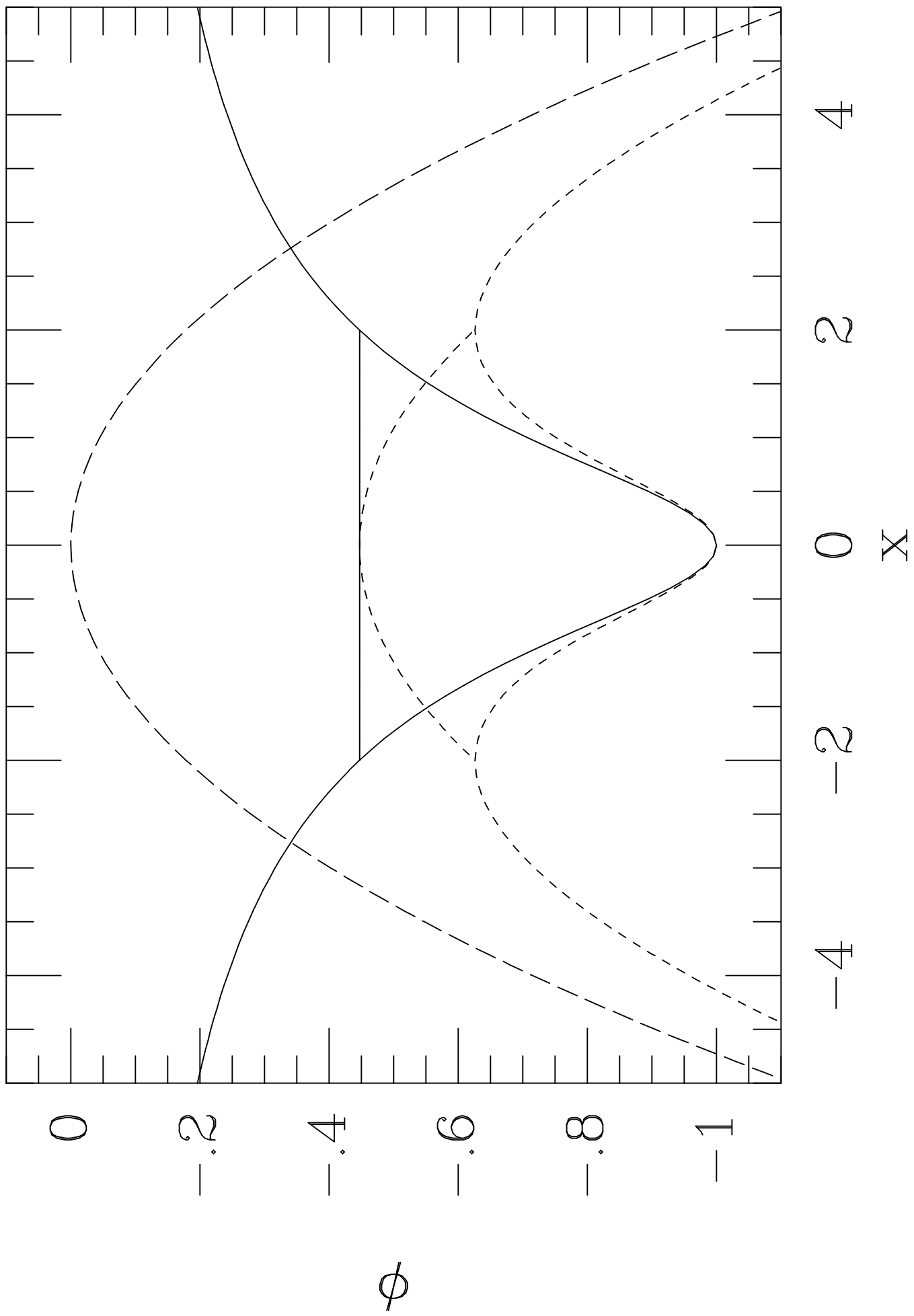
Fig.8. A set of orbits asymptotic to the periodic orbit, all at one energy above E_{crit} . The projection of the phase-space onto the x, y plane is shown.

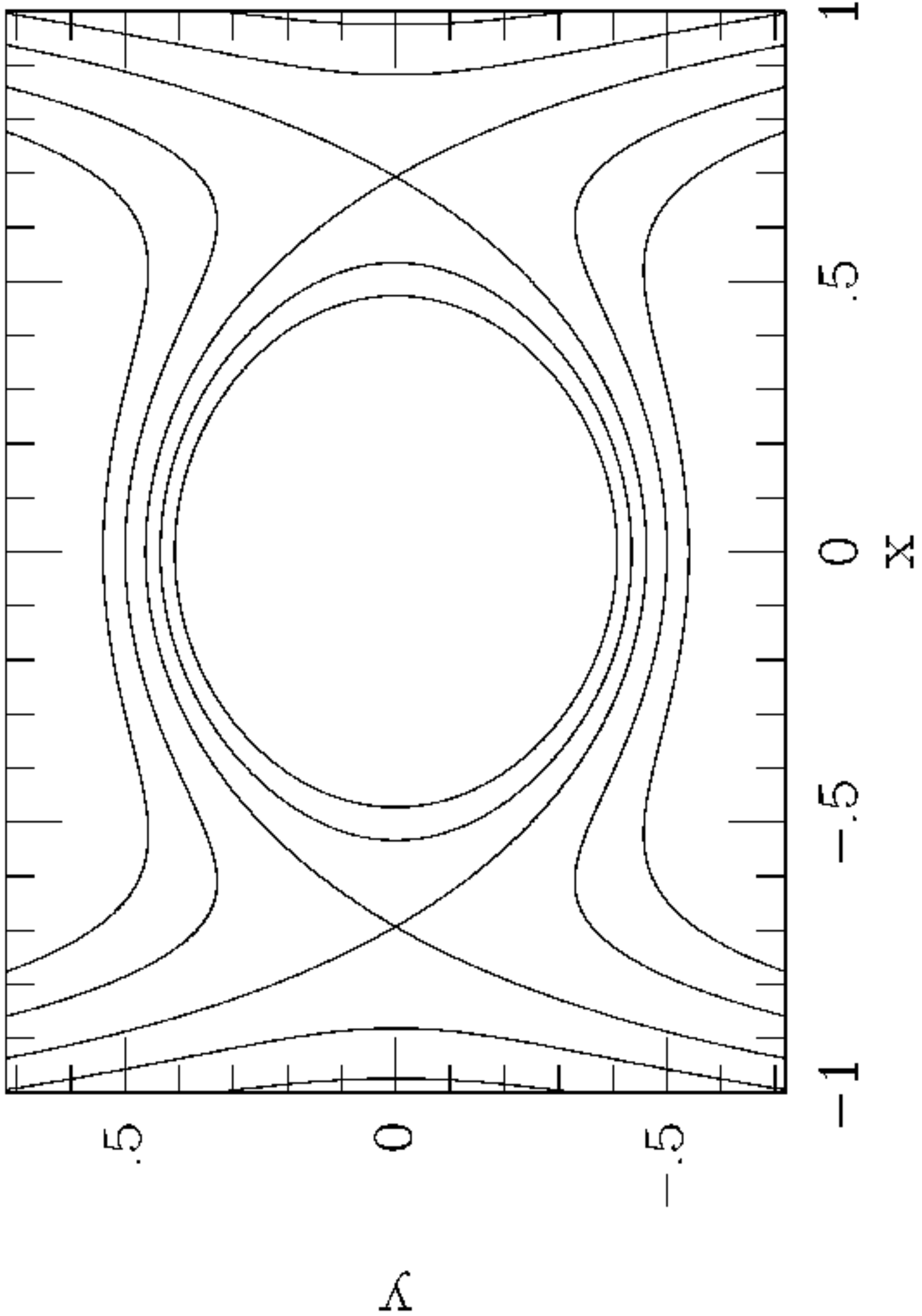
Fig.9 The distribution of the scaled escape time t_s (denoted by \tilde{t} in eq.[11]) for escapers only, in the case of non-uniform initial conditions in a King potential with $W_0 = 3$ (cf. Fig.3). Results are shown as dashed curves for the same values of the scaled energy excess \tilde{E} as in Fig.3. Also shown are the graph of eq.(12), i.e. the long-dashed curve, with t_e

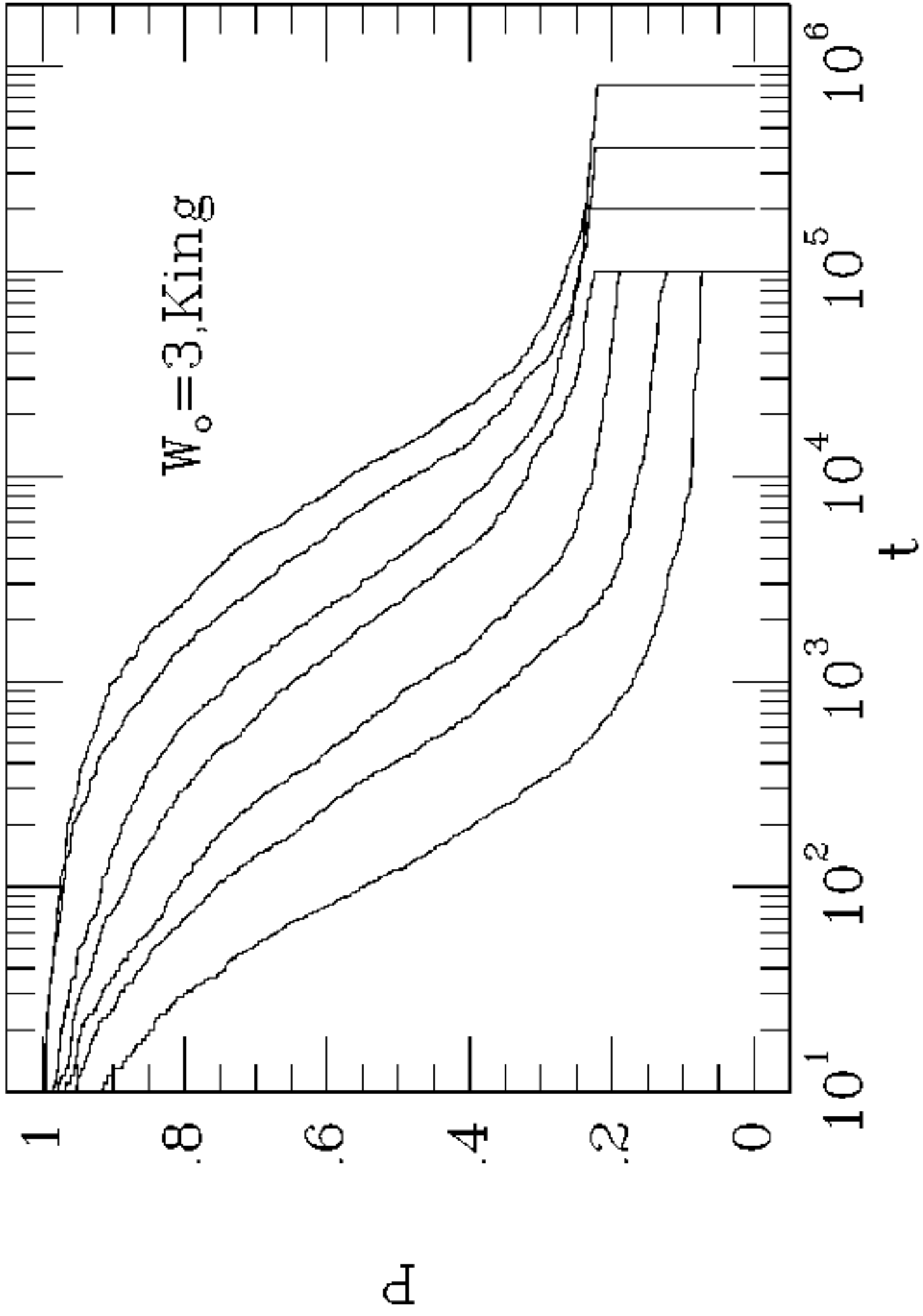
determined as stated in the text, and the empirical fit (solid curve) with parameters from Table 1.

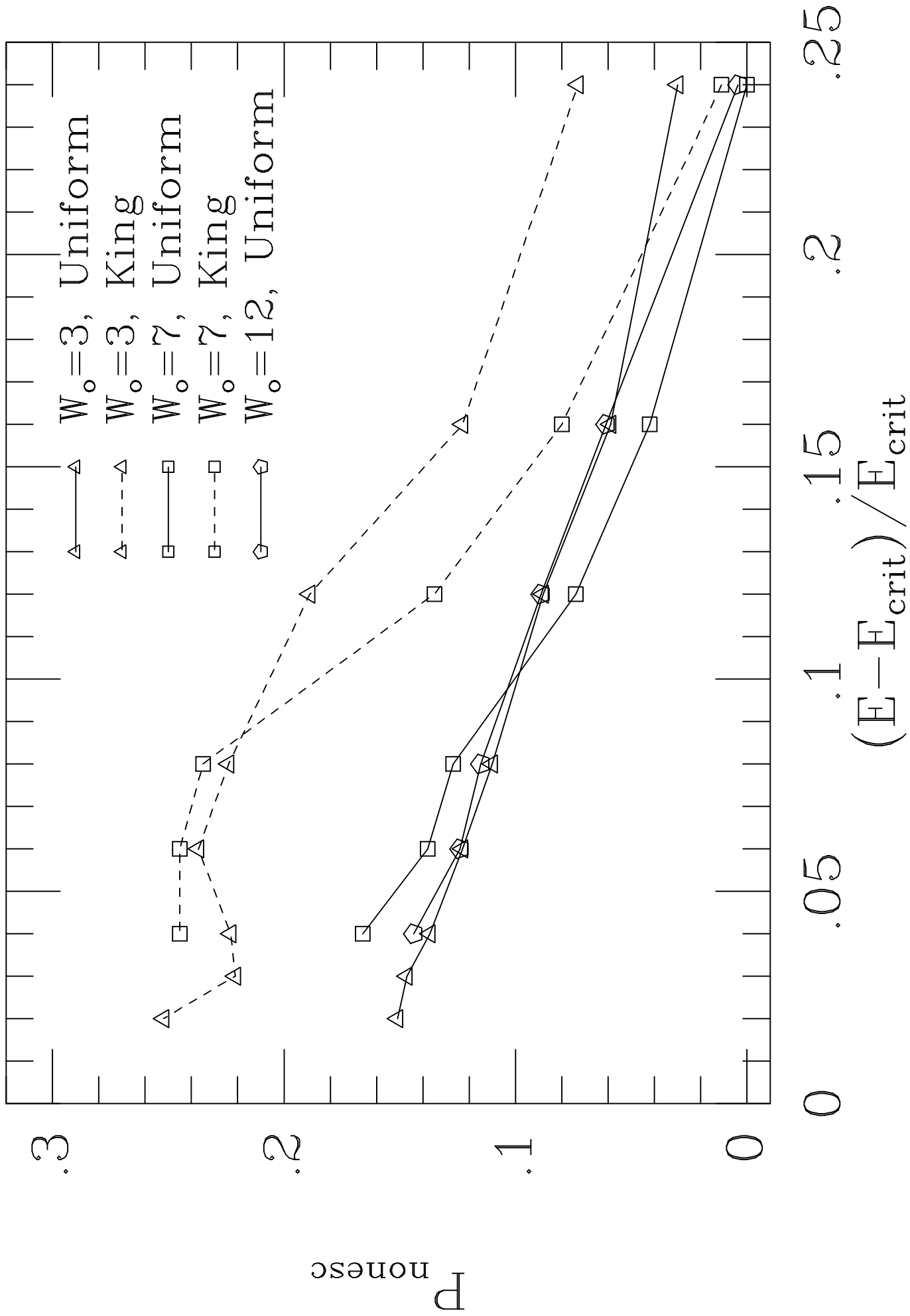
Fig.10 A non-escaper in the potential of a King model with $W_0 = 3$. The orbit is shown every time it crosses the plane $y = 0$ in one direction, by plotting a point with coordinates x (horizontally) and z . Orbits in $x < 0$ are prograde.

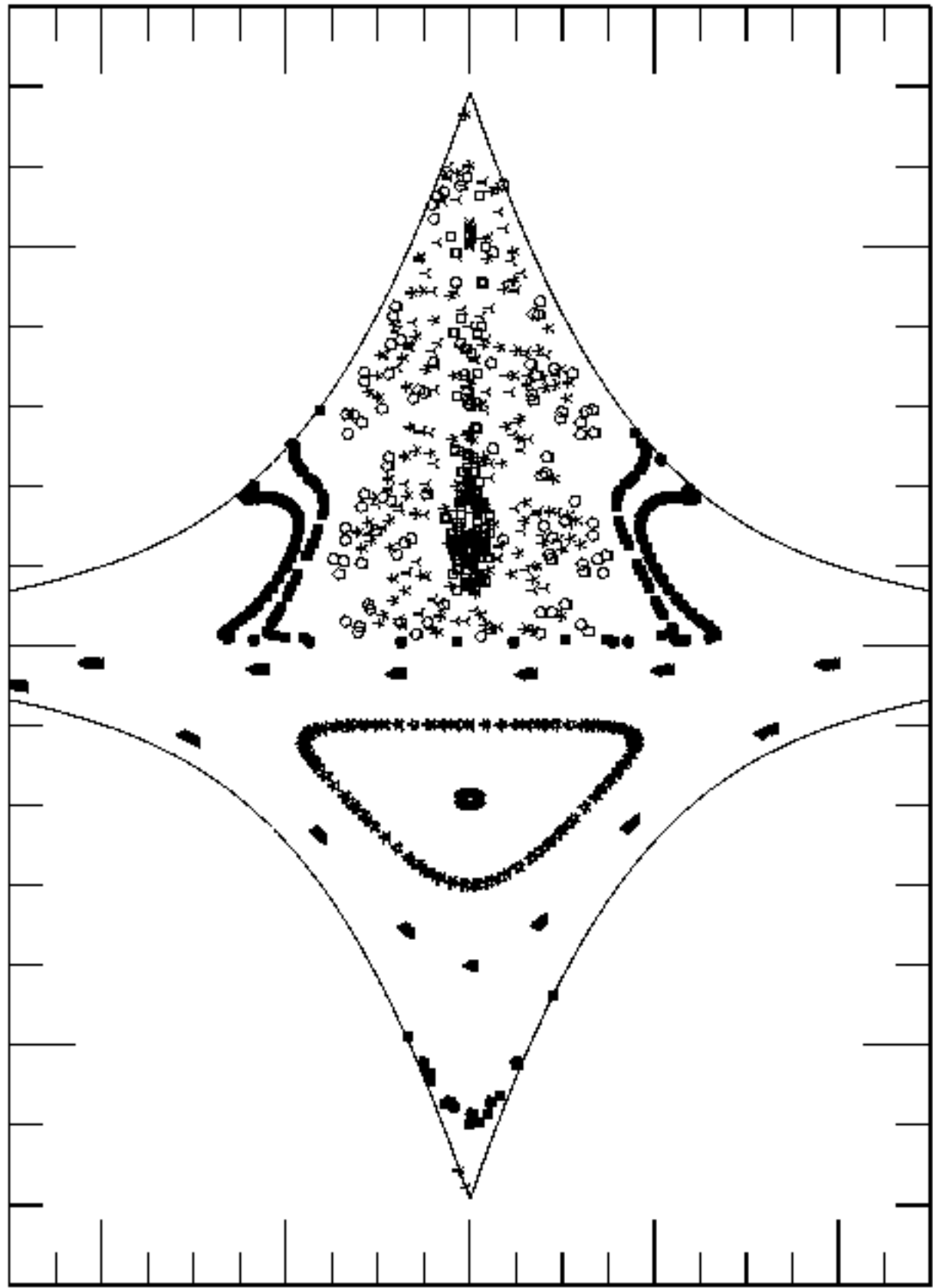
Fig.11 As Fig.10, but for a late escaper. Here $\tilde{E} = 0.04$ and the escape time was 37445.











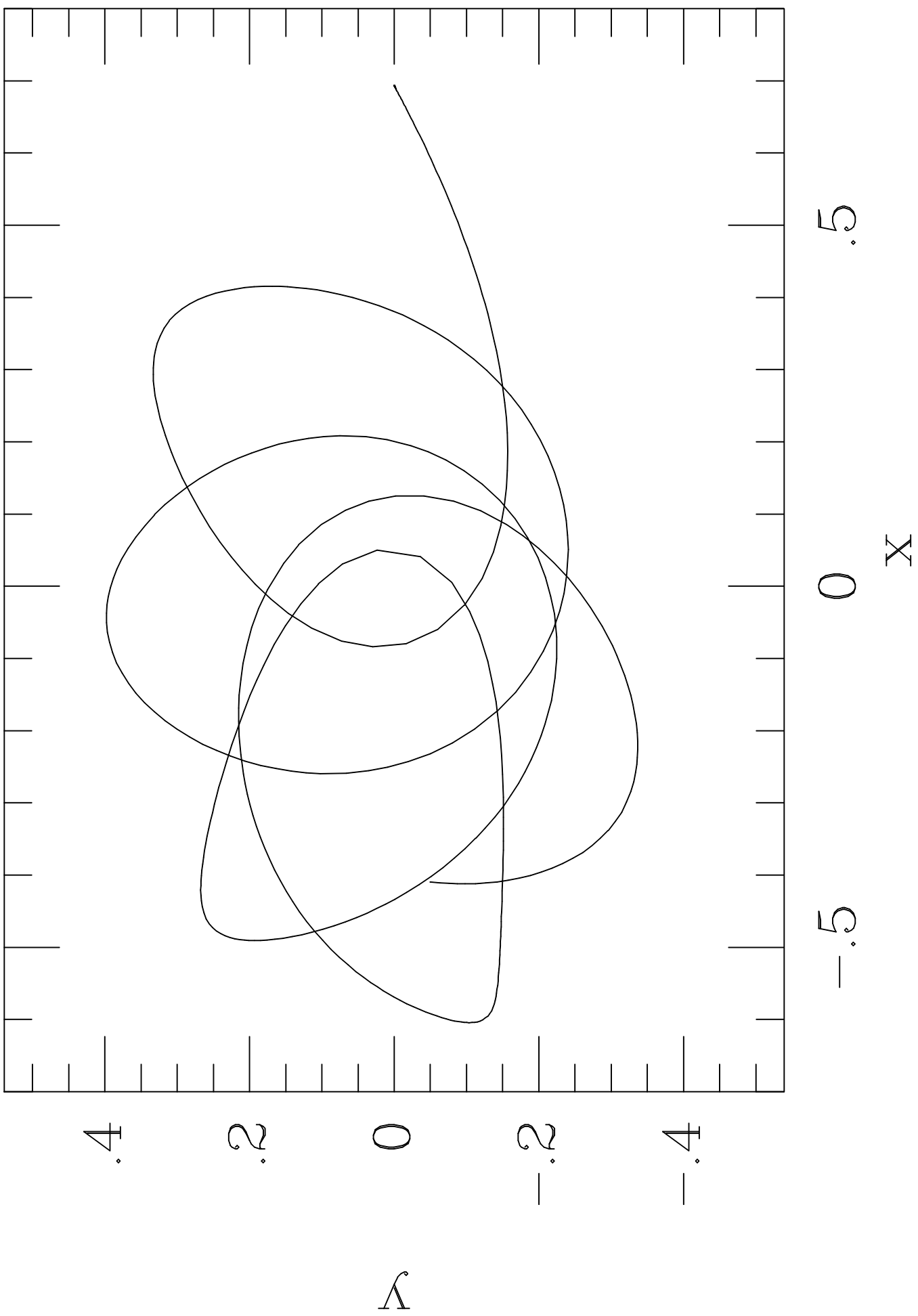
.5

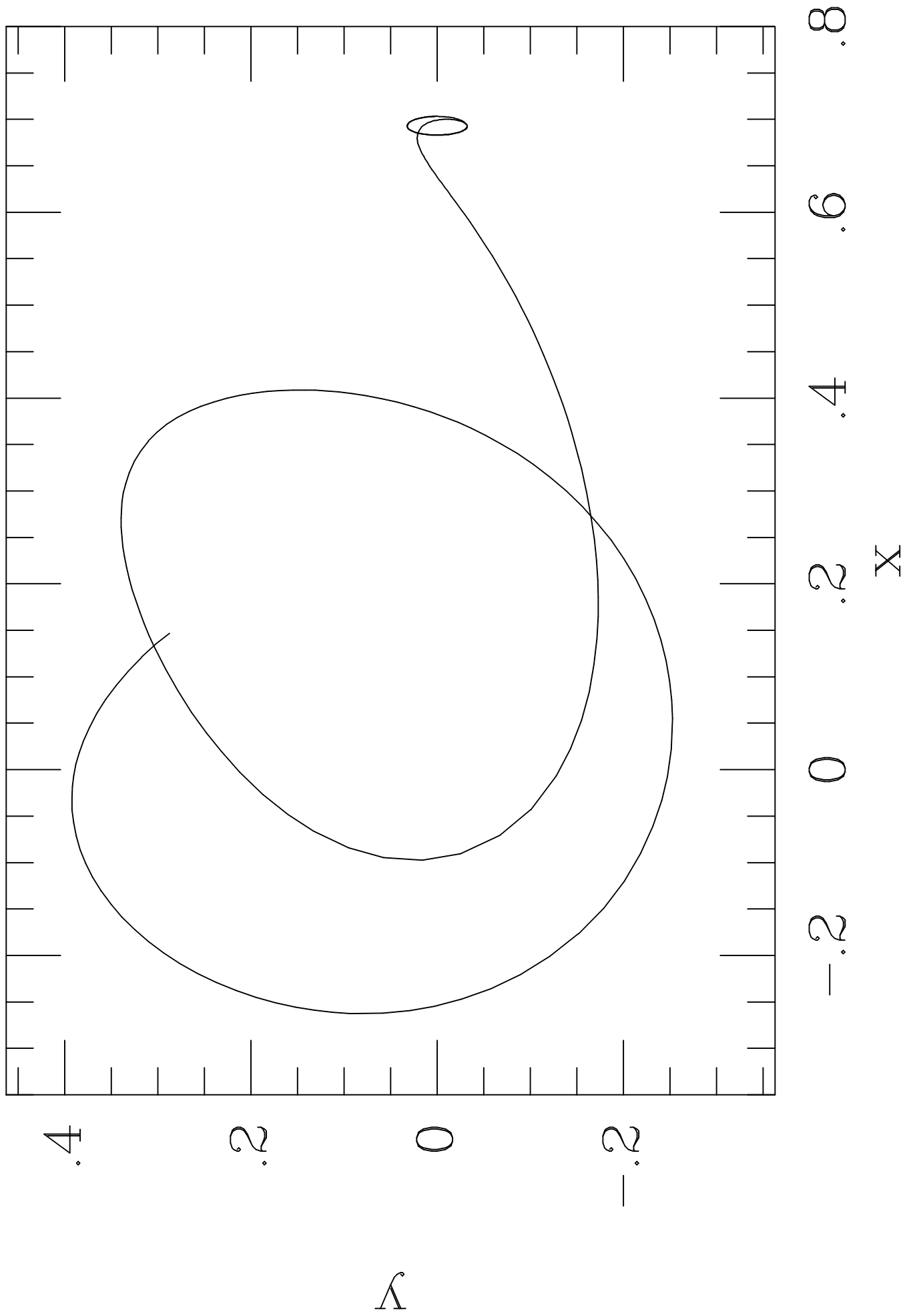
0

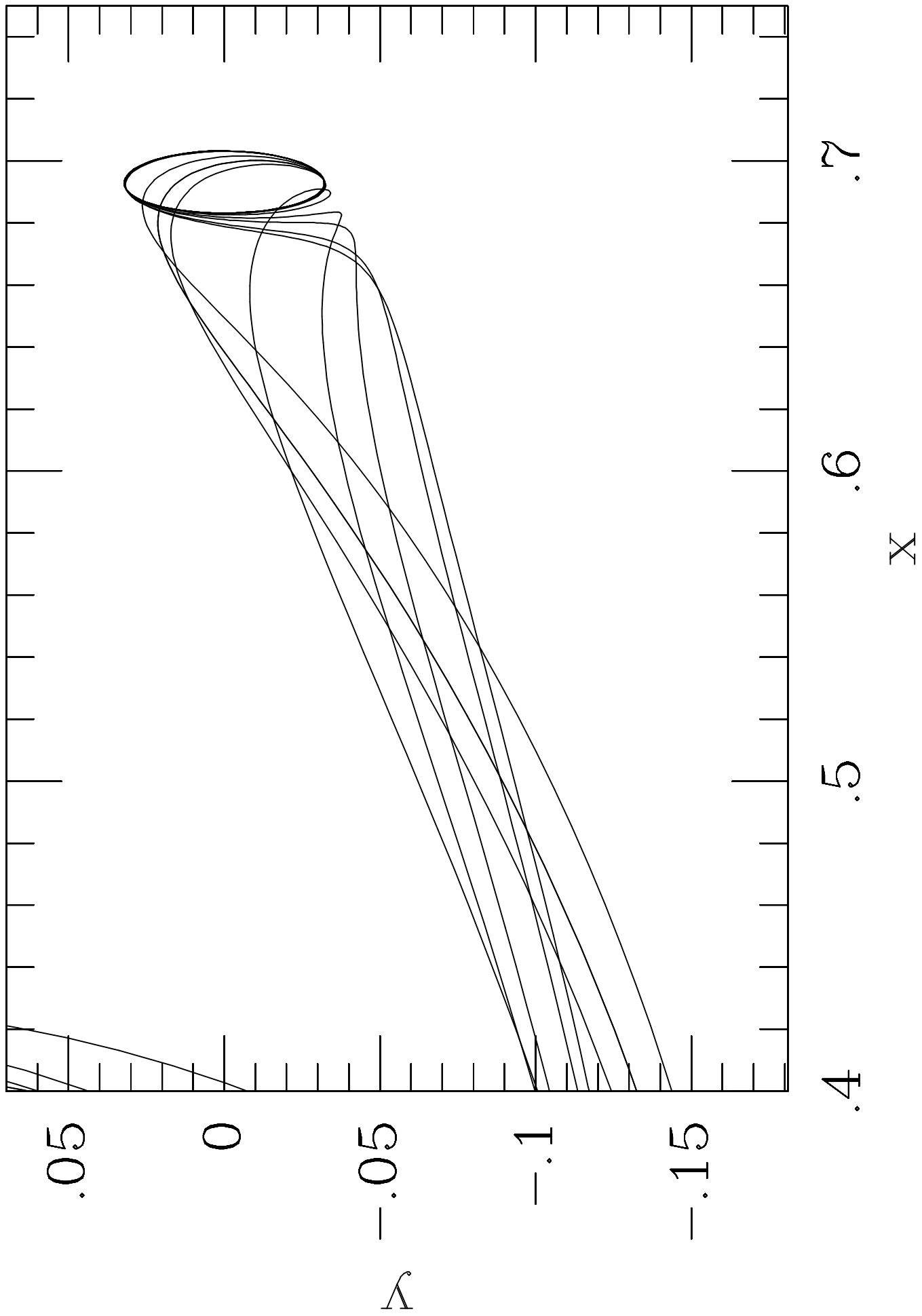
-.5

x

dx/dt







$W_0 = 3, \text{King}$

